



저작자표시-비영리-변경금지 2.0 대한민국

이용자는 아래의 조건을 따르는 경우에 한하여 자유롭게

- 이 저작물을 복제, 배포, 전송, 전시, 공연 및 방송할 수 있습니다.

다음과 같은 조건을 따라야 합니다:



저작자표시. 귀하는 원저작자를 표시하여야 합니다.



비영리. 귀하는 이 저작물을 영리 목적으로 이용할 수 없습니다.



변경금지. 귀하는 이 저작물을 개작, 변형 또는 가공할 수 없습니다.

- 귀하는, 이 저작물의 재이용이나 배포의 경우, 이 저작물에 적용된 이용허락조건을 명확하게 나타내어야 합니다.
- 저작권자로부터 별도의 허가를 받으면 이러한 조건들은 적용되지 않습니다.

저작권법에 따른 이용자의 권리는 위의 내용에 의하여 영향을 받지 않습니다.

이것은 [이용허락규약\(Legal Code\)](#)을 이해하기 쉽게 요약한 것입니다.

[Disclaimer](#)

Uric acid modulates stemness properties of mesenchymal stem cells

Hana Kim

Department of Medical Science
The Graduate School, Yonsei University

Uric acid modulates stemness properties of mesenchymal stem cells

Directed by Professor Phil Hyu Lee

The Doctoral Dissertation
submitted to the Department of Medical Science,
the Graduate School of Yonsei University
in partial fulfillment of the requirements for the degree of Doctor of
Philosophy of Medical Science

Hana Kim

December 2020

This certifies that the Doctoral Dissertation of
Hana Kim is approved.



Thesis Supervisor : Phil Hyu Lee



Thesis Committee Member#1 : Jong Eun Lee



Thesis Committee Member#2 : Han-Soo Kim



Thesis Committee Member#3: Sung-Raë Cho



Thesis Committee Member#4: Se Hoon Kim

The Graduate School
Yonsei University

December 2020

ACKNOWLEDGEMENTS

I would like to express my deep gratitude to Professor Phil Hyu Lee. Attracted by your pure passion for research, I decided to start my Ph.D. program. I wanted to resemble and learn about your passionate side. I was able to come all the way here with your teaching and learned and experienced many things. This paper would not have been possible without your guidance. It was an honor to have a master's and doctorate degree to you.

I would like to thank my committee members, Professor, Jong Eun Lee, Professor, Han-Soo Kim, Professor, Sung-Rae Cho, Professor, Se Hoon Kim, whose work demonstrated to me that concern for global affairs supported by an engagement in neuroscience and taking time to talk with me on many occasions.

I would like to thank the laboratory members for providing indispensable advice, and information. Their assistance and experience helped me complete my thesis. Thank you for spending your precious time with me.

I would like to thank my friends who sympathized with me, comforted me, and listened to my story when I was going through a hard time. I don't think I could have published this paper without them. Thank you for cursing with me, my friends, I love you!

Lastly, mom, dad, and younger brother who always give me infinite love, thank you so much and I love you. I was able to come all the way here because you supported me for a long time and guided me to a good path. Without my reliable family, I couldn't have started or finished studying. Thank you for giving birth to me and raising me as a warm-hearted and right-minded person. Let's walk on the flowery path, my family!

TABLE OF CONTENTS

| | |
|--|----|
| ABSTRACT | 9 |
| | |
| I. INTRODUCTION | 11 |
| II. MATERIALS AND METHODS | 13 |
| 1. MSC and SH-SY5Y cultures | 13 |
| 2. Cell proliferation assay | 14 |
| 3. MSC differentiation and immunostaining | 14 |
| 4. Quantitative real time polymerase chain reaction (RT-PCR) | 15 |
| 5. Western blotting | 17 |
| 6. Reactive oxygen species (ROS) detection and immunostaining | 18 |
| 7. L-lactate assay | 18 |
| 8. Lactate dehydrogenase (LDH) cytotoxicity assay | 18 |
| 9. Uric acid (UA) elevation therapy | 19 |
| 10. Serum urate measurement | 19 |
| 11. Isolation and culture of mouse bone marrow (BM)-MSCs | 19 |
| 12. Animal experiments | 20 |
| 13. Brain sample preparation | 20 |
| 14. Fluorescence activated cell sorting (FACS) | 20 |
| 15. Immunohistochemistry | 21 |
| 16. Stereological cell counts | 21 |
| 17. Rotarod test | 21 |
| 18. Statistical analysis | 22 |
| III. RESULTS | 22 |
| 1. UA enhances glycolysis by upregulating PKM and LDH in MSCs .. | 22 |
| 2. UA regulates stemness and differentiation potential of MSCs | 23 |
| 3. MiR-137 regulates UA-associated MSC priming | 27 |
| 4. Priming MSC with UA exerts neuroprotection in MPP+-treated SH-SY5Y cells | 29 |

| | |
|---|----|
| 5. UA-enhancement therapy augments stemness and differentiation potential of mouse BM-MSCs | 31 |
| 6. MSC priming exerts a neuroprotective effect in MPTP-treated mice | 33 |
| IV. DISCUSSION | 35 |
| V. CONCLUSION | 37 |
| REFERENCES | 38 |
| ABSTRACT (IN KOREAN) | 46 |
| PUBLICATION LIST | 47 |

LIST OF FIGURES

| | |
|---|----|
| Figure 1. UA enhances MSC glycolysis by upregulating PKM and LDH | 23 |
| Figure 2. UA regulates MSC stemness and differentiation potential | 25 |
| Figure 3. miR-137 regulates UA-associated MSC priming | 27 |
| Figure 4. MSC priming with UA exerts neuroprotection in MPP+-treated SH-SY5Y cells | 30 |
| Figure 5. UA-enhancement therapy augments stemness and differentiation potential of mouse BM-MSCs | 32 |
| Figure 6. MSC priming exerts neuroprotection in MPTP-treated mice | 34 |

LIST OF TABLES

| | |
|--|----|
| Table 1. MicroRNAs (miRNAs) associated with self-renewal in stem cells | 29 |
|--|----|

ABSTRACT

Uric acid modulates stemness properties of mesenchymal stem cells

Hana Kim

*Department of Medical Science
The Graduate School, Yonsei University*

(Directed by Professor Phil Hyu Lee)

Parkinson's disease (PD) is characterized pathologically by progressive loss of dopaminergic neurons in the substantia nigra (SN) of the midbrain and the presence of Lewy bodies, proteinaceous fibrillar cytoplasmic inclusions that are composed mainly of aggregated α -synuclein. As a disease-modifying therapy, mesenchymal stem cells (MSCs) are a potential source of cell-based therapy for PD because MSCs secrete various cytotropic factors including neurotrophic growth factors, chemokines, cytokines, and extracellular matrix protein which exert neuroprotective effects. A major challenge in MSCs-based therapy is to develop in vitro culture methods that mimic the natural MSC niche. Cell priming is a promising approach in MSC fate, lineage-specific differentiation, and functions and also enhances their therapeutic potential. Uric acid (UA), a powerful antioxidant, scavenges reactive oxygen species (ROS). ROS generated as the result of cellular metabolism, has a vital role in maintaining stemness and differentiation of MSCs. In the present study, I hypothesized that UA could efficiently decrease ROS levels against oxidative stress, and thus play a central role in maintaining stemness of MSCs. To do this, I evaluated whether MSC priming with UA exerted a more powerful neuroprotective effect in a parkinsonian model and thus provided a practical strategy to improve the application of MSCs in tissue engineering. In vitro, UA treatment in naïve MSCs stimulated glycolysis by upregulating PKM and LDH with no changes in PPP enzymes compared to control MSCs. Low-concentration and short-incubation UA treatment significantly upregulated transcriptional factors responsible for regulation of stemness. After induction with a differentiation medium in MSCs, UA treatment increased the expression levels of osteogenesis-, adipogenesis-, and chondrogenesis-related genes. Similarly, MSCs

that were isolated from animals that received UA-enhancement therapy exhibited increased proliferation properties and increased expression of stemness-related markers OCT4, NANOG, and SOX2 with no changes in expressions of cellular senescence. Priming MSCs with UA increased cellular viability in neurotoxin-treated neuronal cells, relative to naïve MSCs, by inhibiting apoptotic signaling pathways in neurotoxin-induced cellular models. The prosurvival effect of MSCs on dopaminergic neurons in MPTP-treated mice was prominent, with better behavioral recovery of motor deficits in primed MSC-treated mice compared to that in naïve MSC-treated mice. Finally, expression of miR-137 and miR-145 were relatively decreased in UA-treated MSCs compared to that in control MSCs. In summary, priming MSCs with UA exerts neuroprotective properties through enhanced stemness and differentiation potential in parkinsonian models, suggesting a practical strategy for improving the application of MSCs in parkinsonian disorders.

Key words: Parkinson's disease, mesenchymal stem cells, uric acid, priming, stemness

Uric acid modulates stemness properties of mesenchymal stem cells

Hana Kim

*Department of Medical Science
The Graduate School, Yonsei University*

(Directed by Professor Phil Hyu Lee)

I. INTRODUCTION

Parkinson's disease (PD) is characterized pathologically by the progressive loss of dopaminergic neurons in the substantia nigra (SN) and the presence of Lewy bodies, proteinaceous fibrillar cytoplasmic inclusions that are mainly composed of aggregated α -synuclein^{1,2}. The mainstay of PD management is symptomatic treatment with drugs that increase dopamine concentrations or directly stimulate dopamine receptors. Nevertheless, these therapies do not affect the progressive nature of PD and, moreover, they are ineffective against some axial parkinsonian symptoms and various non-motor symptoms. Thus, it is crucial to develop disease-modifying treatments that reduce the rate of neurodegeneration or stop the disease process in α -synucleinopathies.

Stem cell therapy is as one of the most promising novel disease-modifying strategies for PD. The earliest stem cell therapy trials in PD were based on the concept of replacing dopaminergic neurons using human fetal mesencephalic tissue^{3,4}. Thereafter, various sources of dopaminergic neurons, from embryonic stem cells to induced pluripotent stem cells, have been applied to PD animal models, and then, are ready to start clinical trials⁵⁻⁹. However, dopaminergic neuron replacement therapies present many hurdles, including ethical issues, tumorigenesis and mutagenesis, and host-to-graft propagation of α -synuclein^{6,10,11}. Recently, the concept of stem cell therapy has been extended to adult stem cells, which secrete biologically active molecules, exerting beneficial effects on their surroundings¹². Previous studies have shown that mesenchymal stem cells (MSCs) can act as potent modulators of PD-related neurodegenerative microenvironments through the modulation of neuroinflammation, inhibition of apoptosis, increased neurogenesis and neuronal differentiation, enhancement of autophagy, and

modulation of α -synuclein propagation¹³⁻¹⁸. However, the major challenge in MSC-based therapies is to develop in vitro culture systems that mimic the natural MSC niche, while allowing clinical scale cell expansion without compromising quality and function of cell¹⁹. To date, several studies have demonstrated that the modulation of biological, biochemical, and/or biophysical factors can influence the fate, lineage-specific differentiation, functions, and therapeutic potential of MSCs^{20,21}. One approach is cell priming. Many studies have demonstrated the effects of MSC priming with hypoxia, cytokines, growth factors, pharmacological or other chemical agents, biomaterials, and different culture conditions¹⁹. For example, ascorbic acid induces MSC proliferation with upregulation of OCT4 and SOX2²². L-ascorbic acid 2-phosphate, a stable form of ascorbic acid, can maintain the cells in a stable, undifferentiated status without loss of multipotency²³.

Uric acid (UA), a purine metabolite, is a powerful antioxidant, which can be found intracellularly and in all body fluids^{24,25}. It not only scavenges reactive oxygen species (ROS) but also blocks the reaction of the superoxide anion with nitric oxide, which can injure cells by nitrosylating the tyrosine residues of proteins. It also prevents extracellular superoxide dismutase degradation^{26,27}. Ample evidence has suggested that UA has neuroprotective properties in PD, showing that PD patients with higher UA levels have been linked to reduced risk of PD incidence as well as slower disease progression²⁸⁻³⁰. The beneficial effects of UA have also been observed in other neurodegenerative diseases, such as amyotrophic lateral sclerosis³¹, Alzheimer's disease³², and Huntington's disease³³. Hence, UA has not only antioxidant properties but also neuroprotective properties against neurodegenerative conditions.

The functions fulfilled by specialized stem cells, such as stem cell proliferation, lineage specification, and quiescence require a certain energy supply^{34,35}. Glycolysis is the enzymatic conversion of glucose to pyruvate, which generates two net ATP molecules per glucose molecule²⁹. However, cells in oxygen-rich environments may prefer oxidative phosphorylation (OXPHOS), which on average yields 34 additional ATP molecules per glucose by oxidizing pyruvate to acetyl-CoA in the mitochondrial tricarboxylic acid cycle, for a more efficient ATP production²⁹. Many types of stem cells rely on glycolysis when they are undifferentiated, but they activate the mitochondrial OXPHOS process during

differentiation³⁶. Stimulation of glycolysis in pluripotent or adult stem cells by hypoxia or supplementation with insulin promotes stemness, while glycolysis inhibition halts proliferation and induces cell death³⁷. In terms of pluripotency genes, OCT4, NANOG, and SOX2 constitute the core regulatory network that suppresses differentiation-associated genes, thereby maintaining cell pluripotency^{38,39}. OCT4, a key transcription factor essential for self-renewal and survival of MSC interacts with other embryonic regulators, such as SOX2 and NANOG, to regulate the network that maintains pluripotency and inhibits differentiation⁴⁰⁻⁴². Moreover, OCT4 has a number of targets associated with energy metabolism, which may impact the balance between glycolysis and oxidative metabolism⁴³⁻⁴⁵.

ROS resulting from cellular metabolism are crucial for stemness and stem cell differentiation. Differentiation stimuli cause elevated ROS levels, thus inducing stem cell differentiation into specific lineages⁴⁶⁻⁵². However, glycolysis enhancement via hypoxia and OXPHOS suppression, which lead to concomitantly decreased ROS levels, promote stem cell maintenance and proliferation, thereby repressing differentiation^{53,54}. On the other hand, ROS could also lead to stem cell dysfunction, leading to senescence with loss of stemness⁵⁵⁻⁵⁸. Thus, antioxidant would be a core relationship between redox homeostasis and pluripotency of stem cells. In the present study, I hypothesized that UA can efficiently decrease ROS levels against oxidative stress and thus play a central role in stemness maintenance. To prove this, I evaluated whether UA treatment enhances stemness properties in MSCs. Moreover, we tested whether UA-primed MSCs exerts a neuroprotective effect in PD animal models, thus providing a strategy to improve MSC application in tissue engineering.

II. MATERIALS AND METHODS

1. MSC and SH-SY5Y cultures.

Frozen vials of characterized human MSCs at passage two were obtained from the Severance Hospital Cell Therapy Center (Seoul, South Korea; IRB: 4-2008-0643). A human neuroblastoma cell line, SH-SY5Y, was obtained from the Korean Cell Line Bank (Seoul, South Korea). Both MSCs and SH-SY5Y cells were maintained in Dulbecco's modified Eagle medium (DMEM,

HyClone, Irvine, CA, USA), supplemented with 10% fetal bovine serum (FBS; HyClone) and an antibiotic mixture of penicillin and streptomycin (1%, HyClone). When these cells reached 70%–80% confluence, they were trypsinized and subcultured. The cells were cultivated in a humidified incubator at 37°C and 5% CO₂ before use. The MSCs were plated at a density of 1×10^4 per square centimeter. For MSC priming, the cells were treated with either 200 μ M or 400 μ M UA (Sigma, St. Louis, MO, USA), each for 24 hrs and 48 hrs. The SH-SY5Y cells were plated at a density of 2×10^4 per square centimeter and treated with MPP⁺ (100 μ M; Sigma) for 24 hrs. Subsequently, the medium was refreshed, and the cells were cocultured with MSCs or UA-treated MSCs. The MSCs were plated on the permeable membrane of a Costar Transwell insert (Corning, Big Flats, NY, USA), with the SH-SY5Y cells on the bottom of the plate.

2. Cell proliferation assay.

Cell viability was measured using the CellTiter 96[®] Aqueous One Solution Cell Proliferation Assay (Promega, Madison, WI, USA), in accordance with the manufacturer's protocol. Briefly, after the cells were incubated with the various medium samples, MTS(3-(4,5-dimethylthiazol-2-yl)-5-(3-carboxymethoxyphenyl)-2-(4-sulfophenyl)-2H-tetrazolium) was added to a final concentration of 0.5 mg/mL. After incubation at 37°C for 1 h, the plates were centrifuged and the medium was aspirated from each well. The absorbance was measured at 490 nm through an ELISA microplate VersaMax reader (Molecular Devices, Sunnyvale, CA, USA).

3. MSC differentiation and immunostaining.

Osteogenic differentiation was induced by adding ascorbic acid (50 μ g/ml), sodium β -glycerophosphate (10 mM), and dexamethasone (10^{-8} M) to the complete medium. After 2 wks, the plates were washed with phosphate buffered saline (PBS, Sigma), fixed with 4% paraformaldehyde, and stained with 1% alizarin red S (ARS). Adipogenic differentiation was induced by addition of dexamethasone (10^{-7} M) and insulin (6 ng/ml) to the complete medium.

After 3 wks, the plates were washed with PBS, fixed with 4% paraformaldehyde, and stained with Oil red O (ORO). Chondrogenic differentiation was induced by ascorbic acid (50 µg/ml) and TGFβ-1 (1 ng/ml) addition to the complete medium. After 2 wks, the plates were washed with PBS, fixed with 4% paraformaldehyde, and stained with 0.05% alcian blue (AB).

4. Quantitative RT-PCR.

The MSCs were plated at a density of 1×10^5 per square centimeter. Total RNA was extracted from the MSCs using TRIzol[®] reagent (Invitrogen, Carlsbad, CA, USA), in accordance with the manufacturer's protocol. An equal amount of RNA (1 µg), for each experiment, was reverse transcribed using amfiRivert cDNA Synthesis Premix (GenDEPOT, Barker, TX, USA). Subsequently, 2 µL of cDNA were used as a template for RT-PCR with the amfiRivert 1-Step RT-PCR Kit (GenDEPOT). PCR was performed using 10 pmol primers for human p16 (Forward 5'-TCCTGATTGGCGGATAGAGC-3', Reverse 5'-CCCTCGTCGAAAGTCTTCCA-3'), human p21 (Forward 5'-TGGAGACTCTCAGGGTCGAAA-3', Reverse 5'-GGCGTTTGGAGTGGTAGAAATC-3'), human OCT4 (Forward 5'-CCTTCGCAAGCCCTCATTTTC-3', Reverse 5'-GGGCGA GAAGGCAAATCTG-3'), human NANOG (Forward 5'-CCCTCCTCCCATCCCTCATAG-3', Reverse 5'-CCTCGCTGATTAGGCTCCA-3'), human SOX2 (Forward 5'-GAAGGATAAGTACACGCTGCC-3', Reverse 5'-TAACTGTCCATGCGCTGGTTC-3'), human PPARG (Forward 5'-ACTTTGGGATCAGCTCCGTG-3', Reverse 5'-GGAGATGCAGGCTCCACTTT-3'), human RHOA (Forward 5'-GTCCACGGTCTGTCTTCAG-3', Reverse 5'-TTTCCACAGGCTCCATCACC-3'), human SMURF1 (Forward 5'-GCTTTGCAAGGCGCGG-3', Reverse 5'-GAGGTGCACAGAAGCTGGAT-3'), human SMURF2 (Forward 5'-CAAGCTGCGCCTGACAGTA-3', Reverse 5'-GCGGTTGATGGCATTGGAAA-3'), human HAT1 (Forward 5'-GGAAATGGCGGGATTTGGTG-3', Reverse 5'-TGTTGACAGGCTACCAGCAAT-3'), human BMP4 (Forward 5'-CGTCCAAGCTATCTCGAGCC-3', Reverse 5'-ACGACCATCAGCATTCGGTT-3'), human

HK2 (Forward 5'-CCCTGAGGACATCATGCGAG-3', Reverse 5'-GATGGCCTTCCGGATCAGAG-3'), human PFKFB3 (Forward 5'-TGCAACTCTGCCTTATCC-3', Reverse 5'-ATACACCTGCACAGCGTACAG-3'), human G6PD (Forward 5'-TCCCGCATCTCTTTCACTCAC-3', Reverse 5'-AGGAGAGGTGGTGGCGAGTAG-3'), human PGD (Forward 5'-GTCCCACCCTTCCACTTT-3', Reverse 5'-CCATCCTGTAGGCACTCC-3'), human TKT (Forward 5'-CCTGGATGGGGACACCAAAA-3', Reverse 5'-GCGTGAAGAAGGCTGCAAAA-3'), human ALDOA (Forward 5'-TTAACCGGAAACGTCTCCCTG-3', Reverse 5'-TTTGTCCGGTAGCTGTGTG-3'), human PKM (Forward 5'-AGGGAATCACGCCACTGC-3', Reverse 5'-AGCCAGAGAAACCAGCCAAG-3'), human LDH (Forward 5'-TGCTCAGCTCCCAGGTCAC-3', Reverse 5'-GCCTTCAACTCCTTCATGGTCT-3'), human Bcl2 (Forward 5'-TGATTTCTCCTGGCTGTCTC-3', Reverse 5'-TGCATATTTGTTTGGGGCAG-3'), human Bax (Forward 5'-CTGAGCAGATCATGAAGACA-3', Reverse 5'-TCCATGTTACTGTCCAGTTC-3'), human cytochrome c (Forward 5'-ACTCTTACACAGCCGCCAAT-3', Reverse 5'-AGGCAGTGGCCAATTATTACTCA-3'), human GAPDH (Forward 5'-GGTGATGGCATGGACTGTGGT-3', Reverse 5'-AAGGGTCATCATCTCTGCCC-3'), mouse p16 (Forward 5'-GTCGCTTCTTCAGGTTTGG-3', Reverse 5'-AAGAACAGCACGTTTCGAT-3'), mouse p21 (Forward 5'-CACCGTGTTCTTCGACATCAC-3', Reverse 5'-CCAGTGCTCAGAGCACGAAAG-3'), mouse OCT4 (Forward 5'-GAGATATGCAAATCGGAGACC-3', Reverse 5'-GCCTGGAGCACCAAAGTG-3'), mouse NANOG (Forward 5'-GCCCTGAGAAGAAAGAAGAG-3', Reverse 5'-CGTACTGCCCCATACTGGAA-3'), mouse SOX2 (Forward 5'-GAAGGATAAGTACACGCTGCC-3', Reverse 5'-TAACTGTCCATGCGCTGGTTC-3'), mouse PPARG (Forward 5'-ACCTCTGCTGGGGATCTGAA-3', Reverse 5'-ATCACGGAGAGGTCCACAGA-3'), mouse RHOA (Forward 5'-TGTCGGGAGTTGGACTAGCCT-3', Reverse 5'-GGGAACTGGTCCTTGCTGAAG-3'), mouse SMURF1 (Forward 5'-AAGGCTCTGCAAGGCTCTAC-3', Reverse 5'-

CTGCAAAGCCACAGGTTTCC-3'), mouse SMURF2 (Forward 5'-CAAGAGTCCTGCTCGCTCAA-3', Reverse 5'-CCAAGAAATCCAGCACCTTGC-3'), mouse HAT1 (Forward 5'-CCAACACAGCAATCGAGCTG-3', Reverse 5'-CTTCAGGCCCTTGTAACCGA-3'), mouse BMP4 (Forward 5'-GAGCCATTCCGTAGTGCCAT-3', Reverse 5'-ACGACCATCAGCATTTCGGTT-3'), mouse IL-1A (Forward 5'-GAGTCGGCAAAGAAATCAAG-3', Reverse 5'-CAGAGAGAGATGGTCAATGG-3'), mouse IFN γ (Forward 5'-TCCTACCCCAATTTCCAATG-3', Reverse 5'-TTGCCGAGTAGATCTCAAAG-3'), mouse IL-17A (Forward 5'-TCCAGAATGTGAAGGTCAAC-3', Reverse 5'-ACAGAGGGATATCTATCAGGG-3'), mouse IL-4 (Forward 5'-GAGAGAGATCATCGGCATTT-3', Reverse 5'-AAAATATGCGAAGCACCTTG-3'), mouse IL-10 (Forward 5'-AGCCTTATCGGAAATGATCC-3', Reverse 5'-GCTCTATTTTCACAGGGGA-3'), mouse IL-11 (Forward 5'-TGGGGACATGAACTGTGTTTG-3', Reverse 5'-CAGGAGGGATCGGGTTAGGA-3') and mouse GAPDH (Forward 5'-GGTTGACATGACTCAGGCA-3', Reverse 5'-TACGACTGAACCCGCCAGCG-3').

5. Western blotting.

Cells and brain tissues were dissolved in ice-cold RIPA buffer (50 mM Tris-HCl, pH 8.0, with 150 mM sodium chloride, 1% Igepal CA-630, 0.5% sodium deoxycholate, and 0.1% sodium dodecyl sulfate; Sigma) plus a protease inhibitor cocktail (Sigma). The lysates were centrifuged at 4°C for 20 mins (14,000 \times g) and the supernatants transferred to fresh tubes. Briefly, 10 μ g of protein were separated by SDS-gel electrophoresis and transferred onto hydrophobic PVDF membranes (GE Healthcare). The membranes were blocked in nonfat milk (BD) and probed with the following primary antibodies: rabbit anti-p16 (Abcam), rabbit anti-p21 (Abcam), rabbit anti-OCT4 (Cell Signaling), rabbit anti-NANOG (Cell Signaling), rabbit anti-SOX2 (Cell Signaling), rabbit anti-caspase-3 (Cell Signaling), rabbit anti-cleaved caspase-3 (Cell Signaling), and mouse anti-actin (Santa Cruz). As secondary antibodies, horseradish peroxidase-conjugated goat anti-rabbit

(GenDEPOT) and anti-mouse antibody (GenDEPOT) were used at a 1:5000 dilution. Antigen–antibody complexes were visualized with a chemiluminescence system (Santa Cruz). For semiquantitative analysis, immunoblotting band densities were measured by image J.

6. ROS detection and immunostaining.

The intracellular ROS levels were measured through the 2',7'-dichlorodihydrofluorescein diacetate (DCFDA) cellular ROS detection assay kit (Abcam), according to the manufacturer's instructions. For the microplate reader-based assay, a microplate reader (SpectraMax 340PC; Molecular Devices, Inc., Sunnyvale, CA) was used to measure the absorbance at a 485 nm excitation wavelength and a 520 nm emission wavelength, and the data were analyzed using the Softmax Pro software (Molecular Devices). For immunostaining, the cells were washed twice with PBS and fixed in 10% methanol in PBS for 30 mins. After two further washes in PBS, the cell nuclei were counterstained with 4',6-diamidino-2-phenylindole (DAPI; Invitrogen). The immunostained cells were analyzed using bright-field microscopy and viewed under a Zeiss LSM 780 confocal imaging system (Zeiss).

7. L-lactate assay.

The intracellular lactate levels were measured using a colorimetric L-lactate assay kit, according to the manufacturer's instructions (Abcam, ab65330). To eliminate the endogenous LDH, the cell lysates were deproteinized and incubated in the presence of the lactate probe and enzyme mix at room temperature for 30 mins; then, the absorbance was measured using a microplate reader at 570 nm.

8. LDH cytotoxicity assay.

LDH release was measured using the LDH cytotoxicity detection kit (Takara Bio, Shiga, Japan), according to the manufacturer's instructions. The supernatant (100 μ L) and reaction mix (100 μ L) were mixed in 96-well plates and incubated for 30 mins at room temperature. All samples were measured using a microplate reader at 490 nm.

9. UA elevation therapy.

All procedures were performed in accordance with the Laboratory Animals Welfare Act, the Guide for the Care and Use of Laboratory Animals, and the Guidelines and Policies for Rodent Experimentation provided by the Institutional Animal Care and Use Committee (IACUC) at the Yonsei University Health System. Male C57BL/6 mice (Orient Bio) were acclimated in a climate-controlled room with a constant 12/12-hrs light/dark cycle for 1 wk prior to drug administration. To induce the hyperuricemia model, the mice were injected with PO (intraperitoneal injection [i.p.], 250 mg/kg, daily for 4 wks) or IMP (i.p. 500 mg/kg, daily for 4 wks). The mice were randomly divided into three groups (n= 12 per group); (a) control, (b) PO, (c) PO and IMP. All the mice were sacrificed after 4 wks.

10. Serum urate measurement.

Blood samples were collected into EDTA tubes from the vena cava using a syringe. The blood samples were centrifuged at $4,000 \times g$ at 4°C for 20 mins to obtain the serum as a supernatant. Serum samples (approximately 20 μl) were collected from each blood sample. The quantity of serum urate in 3.3 μl of each serum sample was measured using the Urate C-test Wako kit, according to the manufacturer's protocol.

11. Isolation and culture of mouse BM-MSCs.

Mice aged 6 wks were sacrificed by cervical dislocation and placed in a 100-mm cell culture dish (Becton Dickinson, Franklin Lakes, NJ, USA), where the whole body was soaked in 70% (v/v) ethanol for 2 mins. The mouse was then transferred to a new dish. Under sterilized conditions, the fur was washed with 70% alcohol, and the femurs were removed and collected in a petri dish containing the transport medium DMEM. The medium was supplemented with streptomycin (500 mg/mL). Under sterilized conditions, the femurs were cleaned off from the remaining muscle tissues with sterile surgical tools and washed with normal saline solution. The femurs were held

with the forceps, and the knee ends were cut off. A 27-G needle, containing MEM medium supplemented with 20% FBS and 100 mg/mL of each ampicillin and streptomycin, was fit into the bone cavity. The femur was cut off as close as possible to the end. The tip of the bone was inserted into a test tube (15 mL) and the bone marrow was flushed out of the femur. The marrow was dispersed to a suspension by pipetting the large marrow cores. Finally, 10 mL-aliquots of the cell suspension were dispensed into 25-cm² tissue culture flasks, and the cultures were maintained at 37°C in a humidified 95% air and 5% CO₂ incubator. All the samples were processed within 30 mins after sacrifice to ensure high cell viability. The soft tissues were completely dissociated from the bones to avoid contamination.

12. Animal experiments.

To evaluate the modulatory effects of priming MSCs in a PD animal model, the mice were injected with 1-methyl-4-phenyl-1,2,3,6-tetrahydropyridine (MPTP, Sigma; i.p., 30 mg/kg, daily for 14 days). They were then randomly divided into five groups (n= 5 per group)—(a) control, (b) MPTP, (c) MPTP and mouse control MSCs, (d) MPTP and mouse MSCs primed with PO + IMP, and (e) MPTP and human MSCs primed with UA. The mice in the MSC groups were injected with MSCs or primed MSCs via the tail vein (1×10^6 cells per 200 μ l) 3 days after the final MPTP injection. All the mice were sacrificed 4 wks after MSC injection.

13. Brain sample preparation.

For immunochemical analysis, all the mice were deeply anesthetized with chloral hydrate (i.p., 0.4 g/kg; Fluka) and perfused with 4% paraformaldehyde (Sigma) in 0.1 M phosphate buffer (pH 7.4). The brains were embedded in paraffin, and 20 μ m-thick coronal sections were cut and placed on slides.

14. FACS.

The mouse MSCs were characterized by FACS. Briefly, the cell suspensions were washed twice

with PBS containing 0.1% bovine serum albumin (BSA, Sigma). For direct assays, 1×10^6 cells/ml were incubated with phycoerythrin (PE)-conjugated CD44 and anti-human CD105 (positive markers) and fluorescein isothiocyanate (FITC)-conjugated CD34 and CD45 (negative markers) at 4°C for 1 hr and washed twice with PBS containing 0.1% BSA. The cells were analyzed by cytometric analysis using an LSR II flow cytometer (Beckman coulter, San Diego, CA, USA) with BD FACSDiva™ software.

15. Immunohistochemistry.

Deparaffinized brain sections were washed twice in PBS and incubated in 0.2% Triton X-100 (Sigma) for 15 mins at room temperature. They were then blocked with 0.5% bovine serum albumin (BSA; Sigma) for 30 mins. After blocking, they were rinsed three times in 0.25% BSA and incubated overnight at 4°C with a primary mouse anti-tyrosine hydroxylase (TH) antibody (Sigma). The TH antibodies were detected via 0.05% diaminobenzidine (DAB, Vector Laboratories). The immunostained cells were analyzed by brightfield microscopy.

16. Stereological cell counts.

The TH-stained neurons were counted in the SN pars compacta (SNpc) of every fourth section throughout the SNpc. Each midbrain section was first viewed at low power, and the number of TH-stained cells was then counted at high power, starting at a random point. To avoid double counting of neurons with unusual shapes, the TH-stained cells were counted only when their nuclei were optimally visualized, which occurred only in one focal plane. The total number of TH-stained neurons in the SNpc was calculated using the formula described⁷⁹.

17. Rotarod test.

To assess motor function, coordination, and balance, the mice were tested on the Rotarod apparatus (MED-Associates). The day before the training session, the mice were habituated to the apparatus for 15 mins. During the training trials, the mice were trained to run on the rotarod (20 rpm) for 10

mins without falling, twice a day for 3 consecutive days. In the test trials, the mice were placed on the rotarod at 30 rpm (maximum cutoff time: 700 secs). The latency time to fall was recorded.

18. Statistical analysis.

The group means were compared using the Mann–Whitney U test for pairs and the Kruskal–Wallis analysis for multiple groups. $P < 0.05$ was considered statistically significant. All statistical analyses were performed using a commercially available software (SPSS Inc., version 12.0).

III. RESULTS

1. UA enhances glycolysis by upregulating PKM and LDH in MSCs.

To demonstrate whether MSC priming with UA relies on glycolysis, I analyzed the expression levels of rate-limiting enzymes by quantitative RT-PCR. Glucose metabolism consists of interconnected pathways, with key junctions between glycolysis and the pentose phosphate pathway (PPP). A glucose molecule is rapidly phosphorylated to glucose-6-phosphate (G6P) by hexokinase (HK) and is subsequently metabolized toward glycolysis or the PPP (Figure 1A). Compared with the control MSCs, MSCs treated with either 200 or 400 μM UA led to increased mRNA levels of glycolysis enzymes, such as 6-phosphofructo-2-kinase/fructose-2,6-biphosphatase 3 (PFKFB3), pyruvate kinase muscle isozyme (PKM), fructose-bisphosphate aldolase (ALDOA), and lactate dehydrogenase (LDH) (Figure 1B-E). However, the mRNA levels of PPP enzymes, such as glucose 6-phosphate dehydrogenase (G6PD), 6-phosphogluconate dehydrogenase (PGD), and transketolase (TKT), showed no significant differences between UA-treated and control MSCs (Figure 1F-H). Additionally, I examined the concentration of L-lactate, the end product of glycolysis, initial step of which is the conversion of pyruvate to L-lactate by LDH. The L-lactate levels were increased in the UA-treated MSCs compared to those in control MSCs, indicating aerobic glycolysis triggered by UA (Figure 1I). These results demonstrated that UA treatment could stimulate glycolysis by upregulating glycolysis enzymes in MSCs.

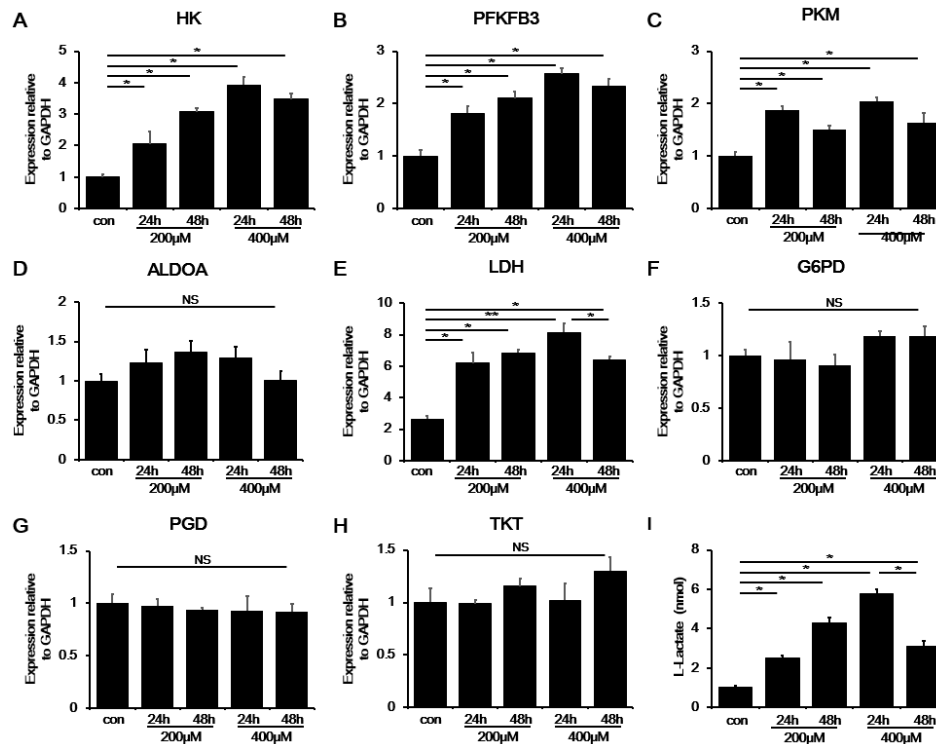


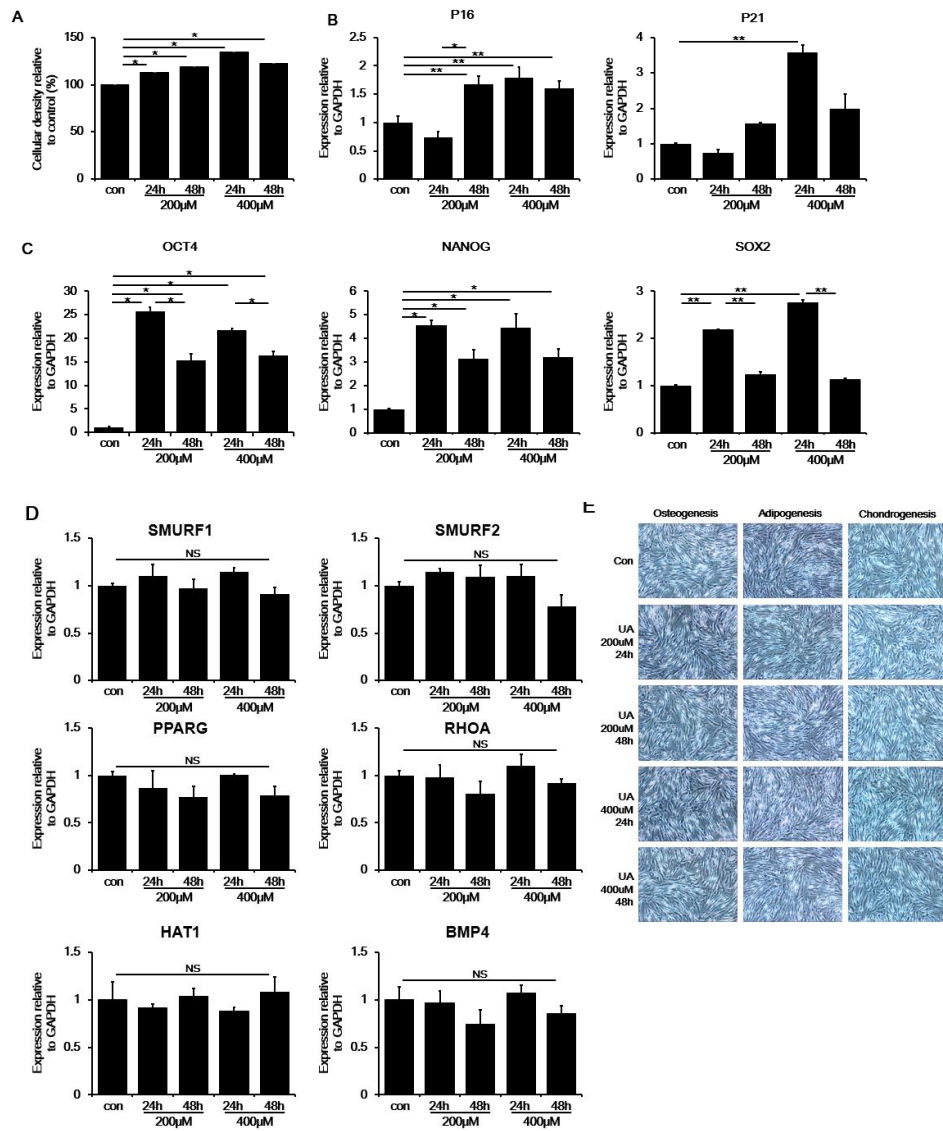
Figure 1. UA enhances MSC glycolysis by upregulating PKM and LDH. (A-E) UA-treated MSCs led to increased mRNA levels of glycolysis enzymes, such as PFKFB3, PKM, ALDOA, and LDH, compared to the control MSCs. (F-H) The mRNA levels of PPP enzymes, such as G6PD, PGD, and TKT, showed no significant differences compared to the control MSCs. (I) L-lactate concentration. UA-treated MSCs presented an increased l-lactate concentration compared to control MSCs. All data are presented as the mean \pm SE. * $p < 0.05$; ** $P < 0.01$.

2. UA regulates stemness and differentiation potential of MSCs.

Next, I examined whether upregulation of glycolysis promotes stemness in UA-treated MSCs. The stem cell properties of MSCs are characterized by their self-renewal ability, high proliferation rate, and multipotent differentiation into osteocytes, adipocytes, and chondrocytes. I performed an MTS analysis to examine whether UA treatment enhances the proliferation properties of the MSCs. UA-treated MSCs showed a significant increase in cellular density compared with control MSCs in a time-dependent manner, regardless of the UA concentration (Figure 2A). Thereafter, to evaluate UA impact on senescence, I analyzed the expression levels of p16 and p21. Expression levels of p16 increased after senescence, whereas those of p21 rapidly increased in cells approaching replicative senescence. Then, the MSCs were treated with 200 μ M or 400 μ M UA, each for 24 hrs and 48 hrs. I

found that the expression levels of p16 and p21 did not increase at an UA concentration of 200 μ M after 24 hrs. However, the expression levels of p16 were increased with an UA concentration of 400 μ M UA after 24 hrs or any UA concentration after 48 hrs. Expression levels of p21 also showed a similar tendency of increased expression, according to UA concentration and incubation time (Figure 2B). These results suggested that UA affects cellular senescence at high concentrations and after long incubation times. Next, I examined the mRNA levels of transcriptional factors responsible for stemness regulation, including OCT4, NANOG, and SOX2. The expression levels of OCT4 increased significantly after 24 hrs of both 200 μ M and 400 μ M UA treatment, whereas they decreased after 48 hrs, regardless of the UA concentration. Similarly, expression levels of NANOG significantly increased after 24 h of 200 μ M and 400 μ M UA treatment and decreased after a 48-h incubation, regardless of the UA concentration. Additionally, expression levels of SOX2 increased after 24 hrs of incubation, whereas they markedly decreased after 48 hrs incubation, independent of UA concentrations (Figure 2C). This indicates that UA enhances stemness in conditions of short incubation and relatively low UA concentrations. Next, to test whether UA-induced stemness augmentation would result in increased differentiation potential of MSCs, I examined the mRNA levels of genes associated with differentiation, including osteogenesis (SMURF1, SMURF2), adipogenesis (PPARG, RHOA), and chondrogenesis (HAT1, BMP4). UA treatment did not affect the expression levels of osteogenesis-, adipogenesis-, and chondrogenesis-related genes in MSCs (Figure 2D). Additionally, I performed ARS, ORO, and AB staining to identify osteogenic, adipogenic, and chondrogenic potential of MSCs, respectively. Immunocytochemistry showed that UA treatment did not affect MSC differential potential toward any lineage (Figure 2E). Moreover, MSCs were cultured with differentiation medium, and then treated at an UA concentration of 200 μ M and 24 hrs. They exhibited increased expression levels of adipogenesis-, osteogenesis- and chondrogenesis-related genes compared with naïve MSCs (Figure 2F). Additionally, immunostaining revealed that UA-treated MSCs after induction with a differentiation medium markedly increased their differentiation potential for osteogenesis, adipogenesis, and chondrogenesis (Figure 2G). Finally, I evaluated whether MSC multipotency was sustained after removal of the UA-containing medium 24 hrs after

UA initiation. Expression levels OCT4, NANOG, and SOX2 that were significantly increased after 24 hrs of UA treatment were dramatically decreased after UA removal (Figure 2H). These data suggest that UA enhances stemness with a strict senescence regulation, depending on its concentration and incubation time.



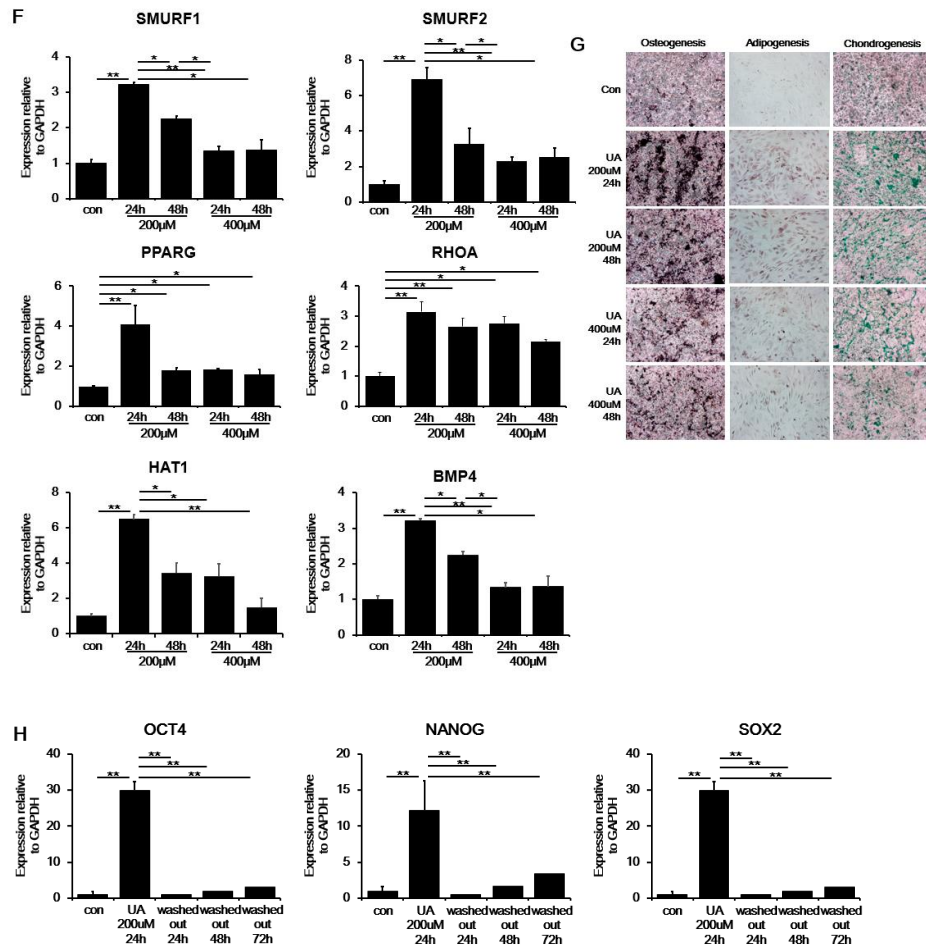


Figure 2. UA regulates MSC stemness and differentiation potential. (A) Cell proliferation assay. UA-treated MSCs showed a significant cell density increase compared to control MSCs in a time-dependent manner, regardless of UA concentration ($n = 3$ per group). (B) Quantitative RT-PCR showed that the expression levels of the senescence markers p16 and p21 did not increase after a 24 hrs incubation with 200 μ M UA. (C) Quantitative RT-PCR showed that the expression levels of the stemness markers OCT4, NANOG, and SOX2 increased after a 24 hrs incubation with 200 μ M UA. (D) Quantitative RT-PCR showed that UA treatment did not affect the expression levels of differentiation markers for osteogenesis (SMURF1, SMURF2), adipogenesis (PPARG, RHOA), and chondrogenesis (HAT1, BMP4). (E) Immunostaining showed that UA treatment did not affect the differentiation potential of MSC in terms of osteogenesis (ARS staining), adipogenesis (ORO staining), and chondrogenesis (AB staining). (F) Quantitative RT-PCR for differentiation markers showed that UA-treated MSCs exhibited increased expression levels of osteogenesis-, adipogenesis-, and

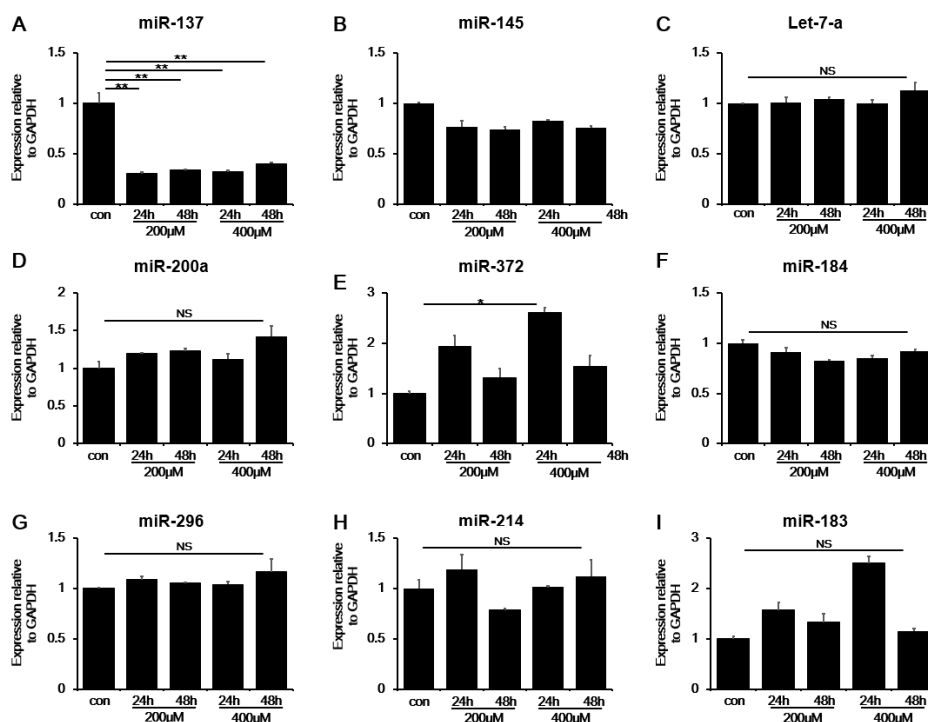
chondrogenesis-related genes compared to naïve MSCs after induction with a differentiation medium.

(G) Immunostaining showed that UA-treated MSCs markedly increased differentiation potential of MSCs toward osteogenesis, adipogenesis, and chondrogenesis after induction with a differentiation medium (H) OCT4, NANOG, and SOX2 expression levels dramatically decreased after UA removal.

All data are presented as the mean \pm SE. * $p < 0.05$; ** $P < 0.01$

3. MiR-137 regulates UA-associated MSC priming

Based on known miRNAs regulating self-renewal in stem cells, I screened 20 miRNAs to uncover possible UA-related stemness-controlling ones (Table 1 and Figure 3A-T). I found that expression levels of miR-137 and miR-145 were decreased in UA-treated MSCs compared to those in control MSCs. Moreover, mRNA levels of miR-137 compared to those of miR-145 levels were markedly decreased in the UA-treated MSCs (Figure 3A and B). The expression levels of the other miRNAs did not differ between UA-treated and control MSCs. These results suggest miR-137 as a candidate regulator of UA-associated MSC priming.



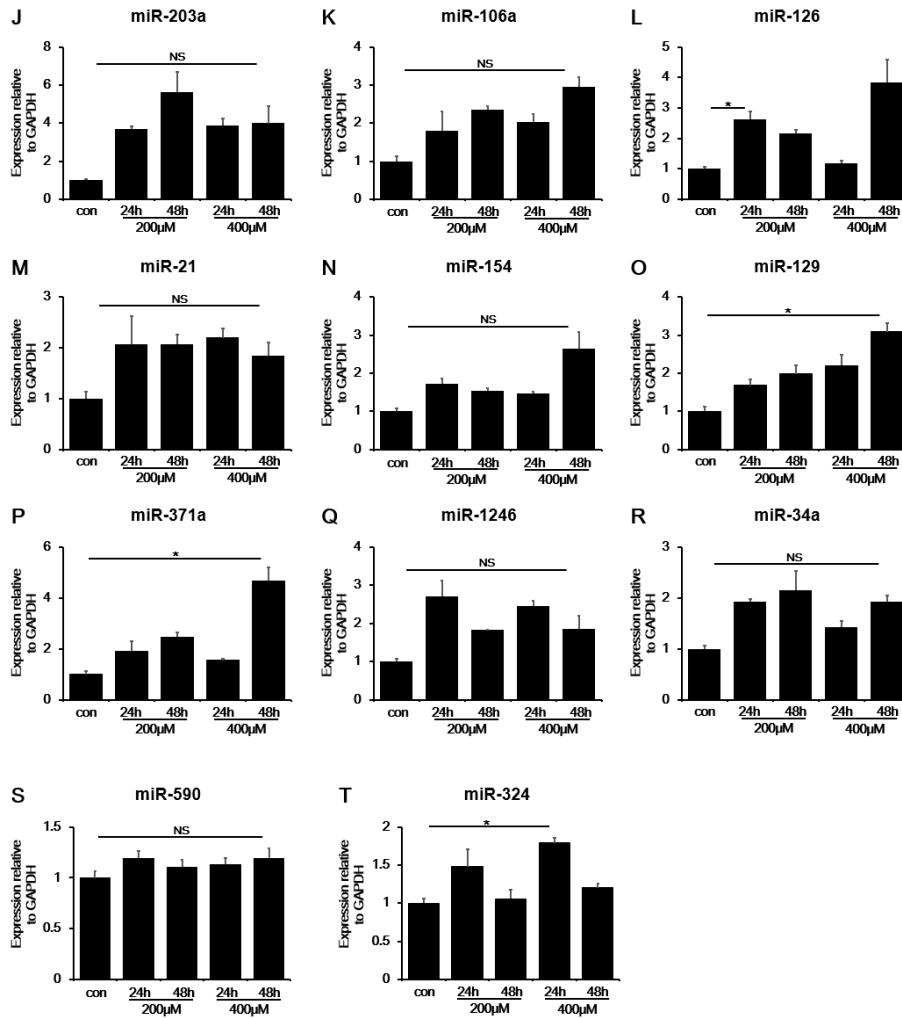


Figure 3. miR-137 regulates UA-associated MSC priming. (A-T) Quantitative RT-PCR for self-renewal related miRNA showed that miR-137 and miR-145 expression levels were decreased in UA-treated MSCs compared to those in control MSCs.

Table 1. miRNAs associated with self-renewal in stem cells

| miRNAs | Sequence | Effects on self-renewal |
|----------|-----------------------------------|-------------------------|
| miR-137 | ACG GGU AUU CUU GGG UGG AUA AU | Promote |
| miR-145 | GUC CAG UUU UCC CAG GAA UCC CU | Promote |
| Let-7-a | UGA GGU AGU AGG UUG UAU AGU U | Maintain |
| miR-200a | CAU CUU ACC GGA CAG UGC UGG A | Promote |
| miR-372 | CCU CAA AUG UGG AGC ACU AUU CU | Promote |
| miR-184 | UGG ACG GAG AAC UGA UAA GGG U | Promote |
| miR-296 | AGG GCC CCC CCU CAA UCC UGU | Promote |
| miR-214 | ACA GCA GGC ACA GAC AGG CAG U | Promote |
| miR-183 | GUG AAU UAC CGA AGG GCC AUA A | Promote |
| miR-203a | AGU GGU UCU UAA CAG UUC AAC AGU U | Inhibition |
| miR-106a | AAA AGU GCU UAC AGU GCA GGU AG | Maintain |
| miR-126 | CAU UAU UAC UUU UGG UAC GCG | Maintain |
| miR-21 | UAG CUU AUC AGA CUG AUG UUG A | Inhibition |
| miR-154 | UAG GUU AUC CGU GUU GCC UUC G | Maintain |
| miR-129 | CUU UUU GCG GUC UGG GCU UGC | Inhibition |
| miR-371a | ACU CAA ACU GUG GGG GCA CU | Promote |
| miR-1246 | AAU GGA UUU UUG GAG CAG G | Promote |
| miR-34a | UGG CAG UGU CUU AGC UGG UUG U | Promote |
| miR-590 | GAG CUU AUU CAU AAA AGU GCA G | Promote |
| miR-324 | CGC AUC CCC UAG GGC AUU GGU G | Inhibition |

4. Priming MSC with UA exerts neuroprotection in MPP⁺-treated SH-SY5Y cells

To examine the effects of UA-associated MSC priming on cell viability, SH-SY5Y cells were treated with MPP⁺ for 24 hrs. Then, the cells were co-cultured with control MSCs, primed MSCs, or primed MSCs with a 24 hrs-UA wash out. MPP⁺ treatment led to a significant decrease in cell survival compared to the control group. However, co-culture of MPP⁺-treated cells with control MSCs, primed MSCs, or primed MSCs with UA wash out in Transwell chambers led to increased cell viability compared to the MPP⁺-treated group. In addition, cell viability was significantly increased in the co-culture group with primed MSCs compared to that with control or primed MSCs with UA wash out (Figure 4A), indicating that UA-primed MSCs has a protective effect. MPP⁺ treatment led to a significant increase in ROS levels, compared to the control group. However, co-culture of MPP⁺-treated cells with control MSCs, primed MSCs, or primed MSCs with UA wash out inhibited ROS generation compared to the MPP⁺-treated group (Figure 4B). In addition, MPP⁺ treatment significantly increased LDH release compared to the control group, whereas co-culture of MPP⁺-treated cells with control MSCs, primed MSCs, or primed MSCs with UA wash out significantly decreased the LDH release, compared to the MPP⁺-treated group (Figure 4C). The modulating effect on ROS and LDH production was more prominent with the primed MSCs than with the control or primed MSCs with UA wash out. Apoptosis analysis revealed that the co-culture

with primed MSCs significantly attenuated cleaved caspase-3 expression compared to the co-culture with control MSCs or primed MSCs with UA wash out (Figure 4D). Moreover, co-culture with primed MSCs induced significantly decreased expression levels of cytochrome C, increased expression levels of Bcl-2, and decreased expression levels of Bax compared to co-culture with control MSCs or primed MSCs with UA wash out (Figure 4E). These results demonstrate that priming MSCs inhibits apoptosis and increases neuronal survival in neurotoxin-treated cells.

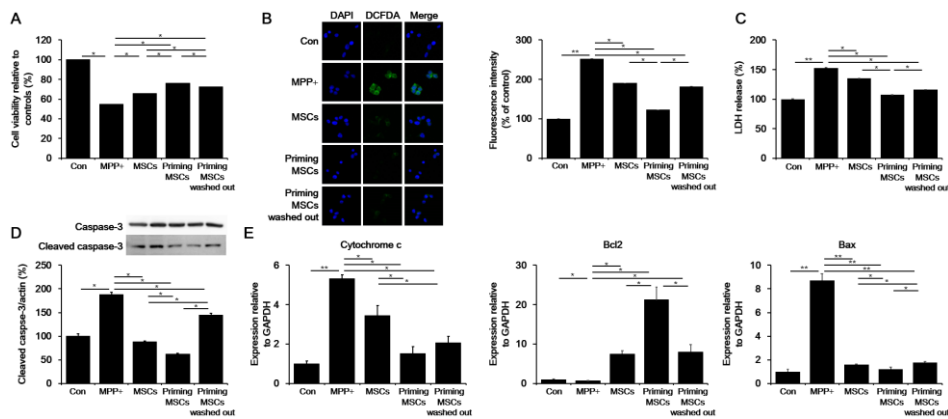


Figure 4. MSC priming with UA exerts neuroprotection in MPP⁺-treated SH-SY5Y cells. (A) MTS analysis showed that co-culture of MPP⁺-treated cells with primed MSCs resulted in significantly increased cell viability compared to the MPP⁺-treated, co-cultured with control MSCs, and co-cultured with primed MSCs with UA wash out groups. (B) ROS activity showed that co-culture of MPP⁺-treated cells with primed MSCs significantly inhibited ROS generation compared to the MPP⁺-treated, co-cultured with control MSCs, and co-cultured with primed MSCs with UA wash out groups. (C) LDH cytotoxicity assay showed that co-culture of MPP⁺-treated cells with primed MSCs significantly inhibited ROS generation compared to the MPP⁺-treated, co-cultured with control MSCs, and co-cultured with primed MSCs with UA wash out groups. (D) Western blotting for apoptosis markers showed that co-culture with primed MSCs significantly attenuated cleaved caspase-3 expression compared to the co-culture with control or primed MSCs with UA wash out. (E) Quantitative RT-PCR for apoptosis markers showed that co-culture with primed MSCs led to significantly decreased cytochrome C, increased Bcl-2, and decreased Bax expression levels compared to the co-culture with control or primed MSCs with UA wash out. All data are presented as the mean ± SE. **p* < 0.05; ***P* <

0.01

5. UA-enhancement therapy augments stemness and differentiation potential of mouse BM- MSCs

To assess whether UA-enhancement therapy increases stemness and differentiation potential of mouse BM MSCs, I injected the mice with potassium oxonate (PO, an uricase inhibitor) and inosine monophosphate precursor (IMP, a precursor of UA) for 4 wks. Serum UA levels were significantly higher in PO- and IMP-treated mice and only PO-treated mice than control mice, but the levels were higher in PO- and IMP-treated mice than in only PO-treated mice (Figure 5A). FACS analysis revealed that the MSCs expressed CD44 and CD105, positive MSC markers, but not CD34 and CD45, negative MSC markers (Figure 5B). The MTS assay showed that the MSC proliferation rate was significantly higher in PO- and IMP-treated mice than in the control or only PO-treated mice (Figure 5C). In addition, I examined the expression levels of p16, p21, OCT4, NANOG, and SOX2 to evaluate whether PO or IMP treatment regulated MSC senescence and stemness. The expression levels of p16 and p21 in PO- and IMP-treated mice did not differ from those in control or only PO-treated mice (Figure 5D). However, the expression levels of OCT4, NANOG, and SOX2 were significantly increased in PO- and IMP-treated mice compared to those in control or only PO-treated mice. Furthermore, the expression levels of these stemness-associated markers were significantly increased in PO-treated mice compared to those in control mice (Figure 5E). Similarly, the mRNA levels of genes associated with osteogenesis (SMURF1, SMURF2), adipogenesis (PPARG, RHOA), and chondrogenesis (HAT1, BMP4) were increased in PO- and IMP-treated mice compared to those in control or only PO-treated mice (Figure 5F). Immunostaining showed that the differentiation potential toward osteogenesis, adipogenesis, and chondrogenesis was markedly increased in PO- and IMP-treated mice compared to that in control or only PO-treated mice (Figure 5G). Next, I examined expression levels of miR-137 and miR-145 to assess whether it is affected by UA-enhancement therapy. The expression levels of miR-137 and miR-145 were relatively reduced in PO- and IMP-treated mice compared to those in control or only PO-treated

mice (Figure 2H). These data suggest that UA-enhancement in mice induces MSC higher proliferation rate and stemness.

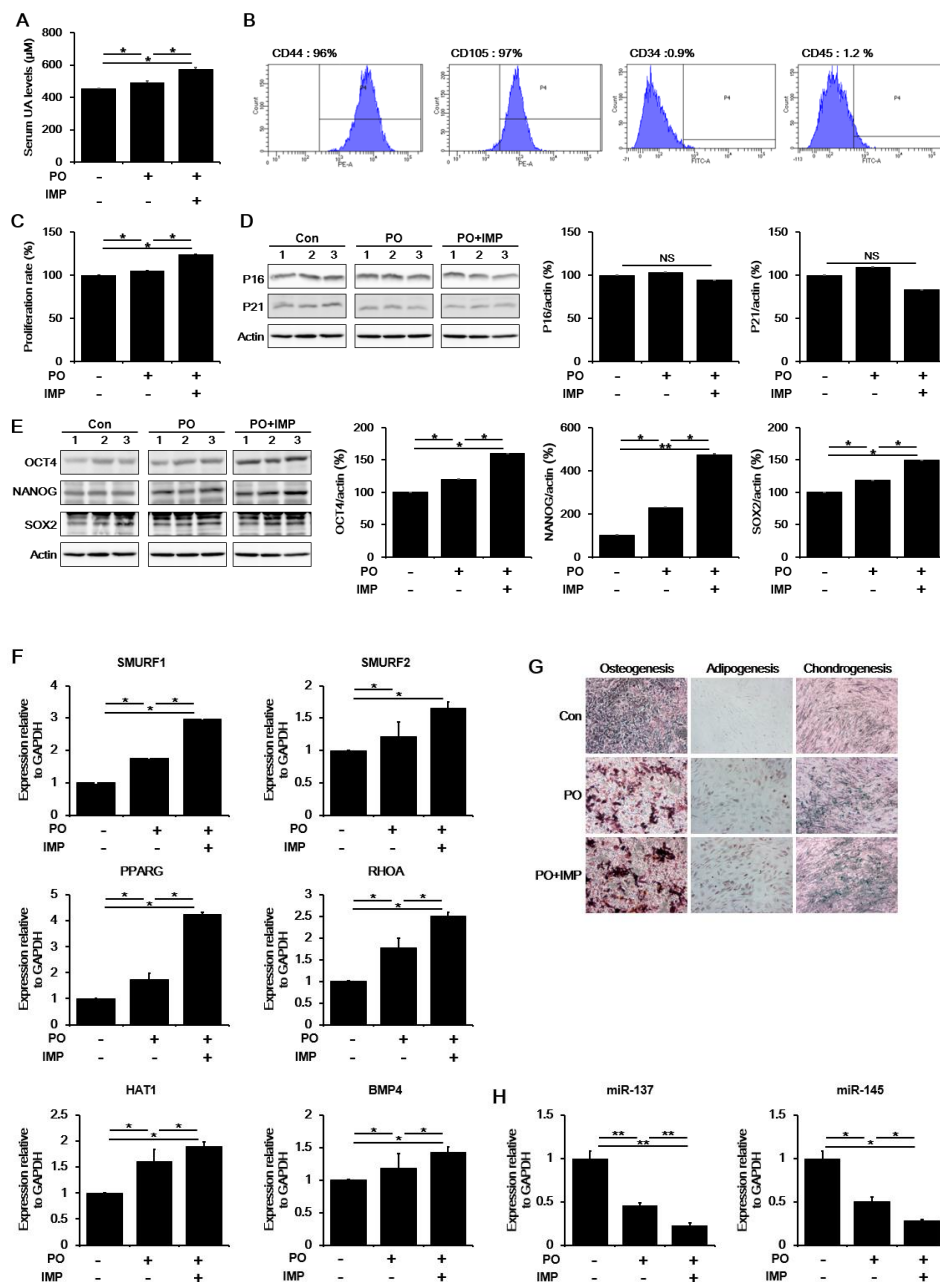


Figure 5. UA-enhancement therapy augments stemness and differentiation potential of mouse BM-MSCs. (A) UA serum levels were significantly higher in PO- and IMP-treated mice than in control or only PO-treated mice. (B) FACS analysis for cell surface markers showed that the MSCs expressed the positive markers CD44 and CD105, but not the negative markers CD34 and CD45. (C) MTS assay showed that MSC proliferation was significantly higher in PO- and IMP-treated mice than in control or only PO-treated mice. (D) Western blotting showed that p16 and p21 expression levels in PO- and IMP-

treated mice did not differ from those in control or only PO-treated mice. (E) Western blotting showed that OCT4, NANOG, and SOX2 expression levels were significantly increased in the PO- and IMP-treated group compared to the control or only PO-treated one. (F) Quantitative RT-PCR for differentiation markers showed that the expression levels of osteogenesis-, adipogenesis-, and chondrogenesis-related genes were increased in PO- and IMP-treated mice compared to those on control or only PO-treated mice. (G) Immunostaining indicated that the differentiation potential of MSCs toward osteogenesis, adipogenesis, and chondrogenesis was markedly increased in the PO- and IMP-treated group compared to the control or only PO-treated group. (H) Quantitative RT-PCR showed that miR-137 and miR-145 expression levels were decreased in PO- and IMP-treated mice compared to those in control or only PO-treated mice. All data are presented as the mean \pm SE. * $p < 0.05$; ** $P < 0.01$

6. MSC priming exerts neuroprotection in MPTP-treated mice

To investigate the potential neuroprotective effects of MSC priming, I performed a comparative analysis of the SN dopaminergic neurons of MPTP-treated parkinsonian mice with different MSC priming conditions. Immunohistochemical analysis revealed a significant decrease in the number of TH-positive neurons in MPTP-treated mice compared to control mice. Any type of MSC treatment increased the survival of TH-positive neurons compared to the MPTP-treated group. Mouse or human MSC priming yielded much higher numbers of TH-positive neurons compared to either the MPTP-treated or the mouse control MSC group (Figure 6A). Consequently, mouse or human MSC priming led to significantly decreased expression levels of cleaved caspase-3 compared to either the MPTP-treated or the mouse control MSC group. Human MSC priming seemed to have a stronger neuroprotective capacity with respect to mouse MSC priming, with the human MSC priming treatment significantly decreasing the expression levels of cleaved caspase-3 (Figure 6B). In addition, I measured the levels of inflammatory cytokines to evaluate the immunomodulatory effects of MSC priming. The levels of pro-inflammatory cytokines, such as interleukin (IL)-1A, IL-17A, and interferon gamma (IFN γ) in MPTP-treated mice were increased compared to those in control mice,

whereas any type of MSC treatment significantly decreased pro-inflammatory cytokine levels in MPTP-treated animals. Similarly, any type of MSC treatment significantly increased the levels of anti-inflammatory cytokines, such as IL-4, IL-10, and IL-11 in MPTP-treated mice (Figure 6C). The cytokine modulating effect was more prominent with mouse or human MSC priming than with mouse control MSC treatment. Consequently, both mouse and human MSC priming treatment led to the restoration of impaired motor coordination and balance on the Rotarod test compared to the control MSC group. Furthermore, human MSC priming showed a higher restorative capacity of impaired motor coordination compared with mouse MSC priming (Figure 6D).

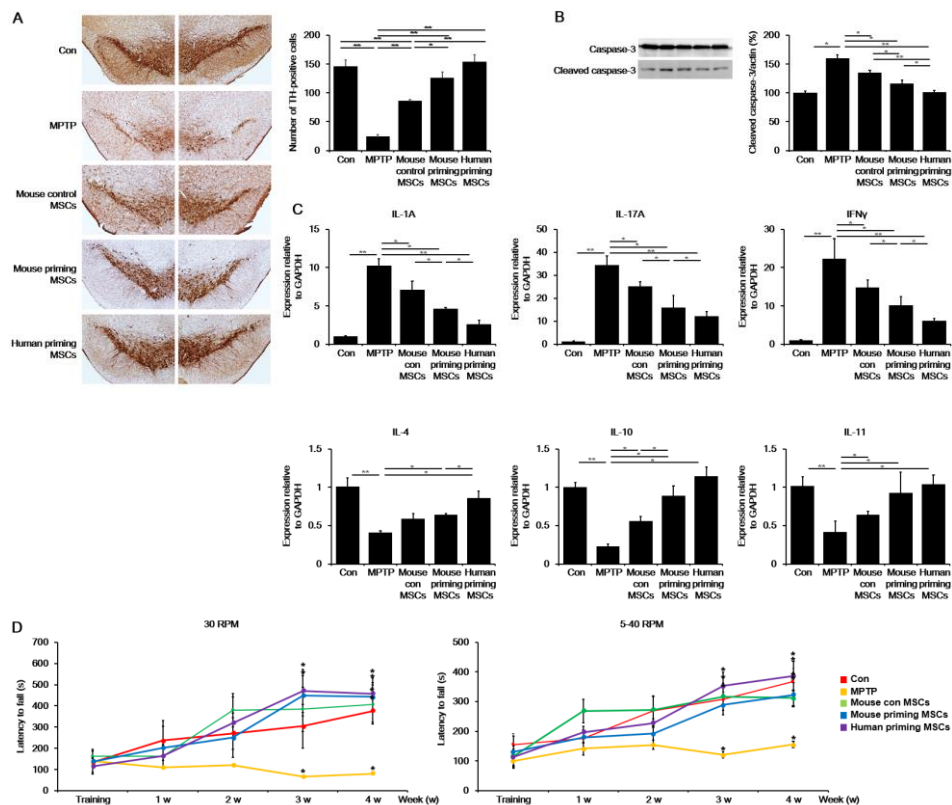


Figure 6. MSC priming exerts neuroprotection in MPTP-treated mice. (A) TH-positive neuron counting in the SN at 4 wks revealed that both mouse and human primed MSC treatment induced much higher numbers of dopaminergic neurons compared to both the MPTP-treated and the mouse control MSC group. (B) Western blotting showed that both mouse and human primed MSC treatment significantly decreased cleaved caspase-3 expression levels compared to both the MPTP-treated and mouse control MSC group. (C) Quantitative RT-PCR showed that both mouse and human primed MSC treatment significantly decreased pro-inflammatory cytokine and increased anti-inflammatory cytokine

expression levels compared to both the MPTP-treated and mouse control MSC group. (D) Both mouse and human primed MSC treatment led to the restoration of impaired motor coordination and balance in the Rotarod test compared to the control MSC group. All data are presented as the mean \pm SE. * $p < 0.05$; ** $P < 0.01$

IV. DISCUSSION

In this study, I investigated the effects of UA on MSC stemness and its neuroprotective action in parkinsonian models. The major findings are as follows: (1) UA treatment increases MSC stemness via glycolysis enhancement by PKM and LDH upregulation, (2) MiR-137 regulates UA-associated MSC priming, (3) UA-primed MSCs exert a more powerful neuroprotective effect in parkinsonian models compared with control MSCs. These data suggest that MSC priming with UA can provide a strategy to improve MSC application to the treatment of parkinsonian disorders.

UA is a final enzymatic product of purine nucleoside degradation in humans. In other mammals, the last enzymatic product of the purine degradation chain is allantoin, which is excreted in the urine⁵⁹. High concentrations of circulating UA were proposed to be the major plasma antioxidant, protecting the cells from oxidative damage. Given that the balance between stem cell self-renewal and differentiation is critical for tissue homeostasis⁶⁰, oxidative stress resulting from excessive ROS production and impaired antioxidant systems can affect proliferation, differentiation, genomic mutations, aging, and death of stem cells⁶¹. Additionally, evidence suggests that redox homeostasis plays a central role in maintaining stemness and reducing stem cell senescence. Thus, disturbances of these mechanisms through excessive ROS production could lead to oxidative stress, resulting in stem cell dysfunction, such as senescence and loss of stemness during long-term expansion^{55,58}. In mammals, stem cells maintain low ROS levels to preserve their stemness and remain quiescent^{57,58,62}. However, research on the link between UA and stemness for clinical applications in neurodegenerative diseases is lacking.

During development, cell fate is defined by transcription factors that act as molecular switches to activate or repress specific gene expression programmes. OCT4, NANOG, and SOX2 are considered

to form a transcriptional regulatory circuitry for pluripotency and self-renewal of stem cells, including MSCs^{41,63}. OCT4 is the most upstream gene in the signaling pathway that regulates MSC self-renewal^{42,63,64}. Thus, the metabolism of undifferentiated MSCs during proliferation is primarily associated with glycolysis^{57,65} under both anaerobic and aerobic conditions^{65,66}, whereas mitochondrial OXPHOS is associated with differentiated MSCs and loss of multipotency⁶⁵. Here, I found that compared with control treatment, UA treatment stimulated glycolysis by upregulating PKM and LDH, with no changes in PPP enzymes. Specifically, glycolysis-related enzymes, such as PFKFB3, PKM, ALDOA, and LDH were significantly upregulated in UA-treated MSCs. In addition, low-concentration and short-incubation UA treatment did not affect MSC senescence, which was accompanied by a significant increase in MSC proliferation properties. mRNA levels in OCT4, NANOG, and SOX2, stemness-related markers, in MSCs were increased by low-concentration and short-incubation UA treatment. However, these conditions did not affect the mRNA levels of genes associated with differentiation, including osteogenesis, adipogenesis, and chondrogenesis, suggesting no impact on the differentiation potential of MSC. UA treatment in lineage-specific differentiated MSCs, nevertheless, exhibited increased expression levels of osteogenesis-, adipogenesis-, and chondrogenesis-related genes, indicating an effect on the differentiation potential of MSC. Moreover, our *in vivo* data further confirmed the impact of UA on MSC stemness modulation. Mice undergoing UA-enhancement therapy showed increased MSC proliferation, and MSCs in IMP- and PO-treated mice exhibited increased expression of OCT4, NANOG, and SOX2, with no changes related to cellular senescence. Our results suggest that UA enhances MSC stemness, with a strict regulation of senescence, possibly depending on UA concentration and incubation time.

MSC priming with UA exerted neuroprotection in neurotoxin-induced parkinsonian cellular and animal models. It significantly increased cell viability in neurotoxin-treated neuronal cells compared to naïve MSCs by inhibiting apoptotic signaling pathways, with concomitant restoration of neurotoxin-induced distorted mitochondrial morphology. *In vivo*, the protective effect of MSCs on dopaminergic neurons in MPTP-treated mice was prominent, regardless of the MSC primed or naïve state. However, the primed MSCs led to the rescue of more SN dopaminergic neurons compared with

naïve MSCs in the MPTP-treated mice. In addition, mice treated with primed MSCs had decreased expression levels of cleaved caspase-3 in the midbrain compared to the mice receiving naïve MSCs. Consequently, motor recovery was prominent in MPTP-treated mice receiving both primed and naïve MSCs, but with a tendency of a better behavioral outcome with the primed MSCs. In terms of species-specific differences in the primed MSCs, human MSCs had more neuroprotective effects than mouse MSCs. Despite many similarities, MSC species variability affects not only the functional expression of various chemokine receptors but also other MSC behaviors⁶⁷⁻⁷⁰. It is possible that species-specific differences may influence MSC priming; however, further studies on this topic are needed.

miRNAs are short non-coding RNAs that post-transcriptionally regulate their target genes⁷¹. Evidence has demonstrated that miRNAs are involved in apoptosis⁷², self-renewal⁷³, and differentiation⁷⁴ of MSCs. Here, I found decreased expression levels of miR-137 and miR-145 in UA-treated MSCs, suggesting that they could promote MSC stemness. Especially, mRNA levels of miR-137 compared to those of miR-145 levels were markedly decreased in the UA-treated MSCs. Decreased expression of miR-137 can lead to increased levels of stemness-related transcriptional factors, including OCT4, NANOG, SOX2, and KLF4^{38,75}, whereas its overexpression induces reduced neural stem cell proliferation, with enhanced neuronal and glial differentiation⁷⁶. miR-137 affects cancer stem cell self-renewal, and its downregulation significantly promoted stemness by targeting KLF12⁷⁷. Furthermore, miR-137 has a critical role in MSC proliferation and differentiation⁷⁶. miR-145 expression was low in self-renewing human embryonic stem cells (ESCs), but it was highly upregulated during differentiation by regulating OCT4, SOX2, and KLF4⁷⁸. Taken together, these results suggest that miR-137 and miR-145 may be closely coupled with MSC stemness regulation by UA.

V. CONCLUSION

MSC priming with UA exerts neuroprotective effects through enhanced stemness and differentiation potential in parkinsonian models. Therefore, this could provide a novel strategy to improve MSC use for the treatment of parkinsonian disorders.

REFERENCES

1. Poewe W, Seppi K, Tanner CM, et al. Parkinson disease. *Nat Rev Dis Primers*. 2017; 3.
2. Goedert M, Spillantini MG, Del Tredici K, Braak H. 100 years of Lewy pathology. *Nat Rev Neurol*. 2013;9(1):13-24.
3. Perlow MJ, Freed WJ, Hoffer BJ, Seiger A, Olson L, Wyatt RJ. Brain grafts reduce motor abnormalities produced by destruction of nigrostriatal dopamine system. *Science*. 1979;204(4393):643-647.
4. Bjorklund A, Stenevi U. Reconstruction of the nigrostriatal dopamine pathway by intracerebral nigral transplants. *Brain Res*. 1979;177(3):555-560.
5. Roy NS, Cleren C, Singh SK, Yang L, Beal MF, Goldman SA. Functional engraftment of human ES cell-derived dopaminergic neurons enriched by coculture with telomerase-immortalized midbrain astrocytes. *Nat Med*. 2006;12(11):1259-1268.
6. Kriks S, Shim JW, Piao J, et al. Dopamine neurons derived from human ES cells efficiently engraft in animal models of Parkinson's disease. *Nature*. 2011;480(7378):547-551.
7. Doi D, Samata B, Katsukawa M, et al. Isolation of human induced pluripotent stem cell-derived dopaminergic progenitors by cell sorting for successful transplantation. *Stem Cell Reports*. 2014;2(3):337-350.
8. Hargus G, Cooper O, Deleidi M, et al. Differentiated Parkinson patient-derived induced pluripotent stem cells grow in the adult rodent brain and reduce motor asymmetry in Parkinsonian rats. *Proc Natl Acad Sci U S A*. 2010;107(36):15921-15926.
9. Sundberg M, Bogetofte H, Lawson T, et al. Improved cell therapy protocols for Parkinson's disease based on differentiation efficiency and safety of hESC-, hiPSC-, and non-human primate iPSC-derived dopaminergic neurons. *Stem Cells*. 2013;31(8):1548-1562.
10. Kirkeby A, Grealish S, Wolf DA, et al. Generation of regionally specified neural progenitor cells from human pluripotent stem cells. *Nat Protoc*. 2014;9(1):1-12.

- nitors and functional neurons from human embryonic stem cells under defined conditions. *Cell Rep.* 2012;1(6):703-714.
11. Grealish S, Diguett E, Kirkeby A, et al. Human ESC-derived dopamine neurons show similar preclinical efficacy and potency to fetal neurons when grafted in a rat model of Parkinson's disease. *Cell Stem Cell.* 2014;15(5):653-665.
 12. Caplan AI, Dennis JE. Mesenchymal stem cells as trophic mediators. *J Cell Biochem.* 2006;98(5):1076-1084.
 13. Oh SH, Kim HN, Park HJ, Shin JY, Lee PH. Mesenchymal Stem Cells Increase Hippocampal Neurogenesis and Neuronal Differentiation by Enhancing the Wnt Signaling Pathway in an Alzheimer's Disease Model. *Cell Transplant.* 2015;24(6):1097-1109.
 14. Kim YJ, Park HJ, Lee G, et al. Neuroprotective effects of human mesenchymal stem cells on dopaminergic neurons through anti-inflammatory action. *Glia.* 2009;57(1):13-23.
 15. Park HJ, Bang G, Lee BR, Kim HO, Lee PH. Neuroprotective effect of human mesenchymal stem cells in an animal model of double toxin-induced multiple system atrophy parkinsonism. *Cell Transplant.* 2011;20(6):827-835.
 16. Park HJ, Shin JY, Kim HN, Oh SH, Lee PH. Neuroprotective effects of mesenchymal stem cells through autophagy modulation in a parkinsonian model. *Neurobiol Aging.* 2014;35(8):1920-1928.
 17. Park HJ, Shin JY, Lee BR, Kim HO, Lee PH. Mesenchymal stem cells augment neurogenesis in the subventricular zone and enhance differentiation of neural precursor cells into dopaminergic neurons in the substantia nigra of a parkinsonian model. *Cell Transplant.* 2012;21(8):1629-1640.
 18. Shin JY, Park HJ, Kim HN, et al. Mesenchymal stem cells enhance autophagy and increase beta-amyloid clearance in Alzheimer disease models. *Autophagy.* 2014;10(1):32-44.
 19. Noronha NC, Mizukami A, Caliari-Oliveira C, et al. Priming approaches to improve t

- he efficacy of mesenchymal stromal cell-based therapies. *Stem Cell Res Ther.* 2019;10(1):131.
20. Huang C, Dai J, Zhang XA. Environmental physical cues determine the lineage specification of mesenchymal stem cells. *Biochim Biophys Acta.* 2015;1850(6):1261-1266.
 21. Nava MM, Raimondi MT, Pietrabissa R. Controlling self-renewal and differentiation of stem cells via mechanical cues. *J Biomed Biotechnol.* 2012;2012:797410.
 22. Potdar PD, D'Souza SB. Ascorbic acid induces in vitro proliferation of human subcutaneous adipose tissue derived mesenchymal stem cells with upregulation of embryonic stem cell pluripotency markers Oct4 and SOX 2. *Hum Cell.* 2010;23(4):152-155.
 23. Yu J, Tu YK, Tang YB, Cheng NC. Stemness and transdifferentiation of adipose-derived stem cells using L-ascorbic acid 2-phosphate-induced cell sheet formation. *Biomaterials.* 2014;35(11):3516-3526.
 24. Becker BF. Towards the physiological function of uric acid. *Free Radic Biol Med.* 1993;14(6):615-631.
 25. Ames BN, Cathcart R, Schwiers E, Hochstein P. Uric acid provides an antioxidant defense in humans against oxidant- and radical-caused aging and cancer: a hypothesis. *Proc Natl Acad Sci U S A.* 1981;78(11):6858-6862.
 26. Squadrito GL, Cueto R, Splenser AE, et al. Reaction of uric acid with peroxynitrite and implications for the mechanism of neuroprotection by uric acid. *Arch Biochem Biophys.* 2000;376(2):333-337.
 27. Kuzkaya N, Weissmann N, Harrison DG, Dikalov S. Interactions of peroxynitrite with uric acid in the presence of ascorbate and thiols: implications for uncoupling endothelial nitric oxide synthase. *Biochem Pharmacol.* 2005;70(3):343-354.
 28. Li X, Jia S, Zhou Z, et al. Effect of serum uric acid on cognition in patients with idiopathic REM sleep behavior disorder. *J Neural Transm (Vienna).* 2018;125(12):1805-1812.
 29. Teslaa T, Teitell MA. Pluripotent stem cell energy metabolism: an update. *EMBOJ.* 20

- 15;34(2):138-153.
30. Tana C, Ticinesi A, Prati B, Nouvenne A, Meschi T. Uric Acid and Cognitive Function in Older Individuals. *Nutrients*. 2018;10(8).
 31. Bakshi R, Xu Y, Mueller KA, et al. Urate mitigates oxidative stress and motor neuron toxicity of astrocytes derived from ALS-linked SOD1(G93A) mutant mice. *Mol Cell Neurosci*. 2018;92:12-16.
 32. Ya BL, Liu Q, Li HF, et al. Uric Acid Protects against Focal Cerebral Ischemia/Reperfusion-Induced Oxidative Stress via Activating Nrf2 and Regulating Neurotrophic Factor Expression. *Oxid Med Cell Longev*. 2018;2018:6069150.
 33. Auinger P, Kiebertz K, McDermott MP. The relationship between uric acid levels and Huntington's disease progression. *Mov Disord*. 2010;25(2):224-228.
 34. Folmes CD, Dzeja PP, Nelson TJ, Terzic A. Metabolic plasticity in stem cell homeostasis and differentiation. *Cell Stem Cell*. 2012;11(5):596-606.
 35. Burgess RJ, Agathocleous M, Morrison SJ. Metabolic regulation of stem cell function. *J Intern Med*. 2014;276(1):12-24.
 36. Varum S, Rodrigues AS, Moura MB, et al. Energy metabolism in human pluripotent stem cells and their differentiated counterparts. *PLoS One*. 2011;6(6):e20914.
 37. Kondoh H, Leonart ME, Nakashima Y, et al. A high glycolytic flux supports the proliferative potential of murine embryonic stem cells. *Antioxid Redox Signal*. 2007;9(3):293-299.
 38. Boyer LA, Lee TI, Cole MF, et al. Core transcriptional regulatory circuitry in human embryonic stem cells. *Cell*. 2005;122(6):947-956.
 39. Wang Z, Oron E, Nelson B, Razis S, Ivanova N. Distinct lineage specification roles for NANOG, OCT4, and SOX2 in human embryonic stem cells. *Cell Stem Cell*. 2012;10(4):440-454.
 40. Jaenisch R, Young R. Stem cells, the molecular circuitry of pluripotency and nuclear reprogramming. *Cell*. 2008;132(4):567-582.

41. Greco SJ, Liu K, Rameshwar P. Functional similarities among genes regulated by OCT 4 in human mesenchymal and embryonic stem cells. *Stem Cells*. 2007;25(12):3143-3154.
42. Lu Y, Qu H, Qi D, et al. OCT4 maintains self-renewal and reverses senescence in human hair follicle mesenchymal stem cells through the downregulation of p21 by DNA methyltransferases. *Stem Cell Res Ther*. 2019;10(1):28.
43. Shakya A, Cooksey R, Cox JE, Wang V, McClain DA, Tantin D. Oct1 loss of function induces a coordinate metabolic shift that opposes tumorigenicity. *Nat Cell Biol*. 2009;11(3):320-327.
44. Chen X, Xu H, Yuan P, et al. Integration of external signaling pathways with the core transcriptional network in embryonic stem cells. *Cell*. 2008;133(6):1106-1117.
45. Kang J, Shakya A, Tantin D. Stem cells, stress, metabolism and cancer: a drama in two acts. *Trends Biochem Sci*. 2009;34(10):491-499.
46. Smith J, Ladi E, Mayer-Proschel M, Noble M. Redox state is a central modulator of the balance between self-renewal and differentiation in a dividing glial precursor cell. *Proc Natl Acad Sci U S A*. 2000;97(18):10032-10037.
47. Lee NK, Choi YG, Baik JY, et al. A crucial role for reactive oxygen species in RANKL-induced osteoclast differentiation. *Blood*. 2005;106(3):852-859.
48. Li J, Stouffs M, Serrander L, et al. The NADPH oxidase NOX4 drives cardiac differentiation: Role in regulating cardiac transcription factors and MAP kinase activation. *Mol Biol Cell*. 2006;17(9):3978-3988.
49. Schmelter M, Ateghang B, Helmig S, Wartenberg M, Sauer H. Embryonic stem cells utilize reactive oxygen species as transducers of mechanical strain-induced cardiovascular differentiation. *FASEB J*. 2006;20(8):1182-1184.
50. Vieira HL, Alves PM, Vercelli A. Modulation of neuronal stem cell differentiation by hypoxia and reactive oxygen species. *Prog Neurobiol*. 2011;93(3):444-455.
51. Chaudhari P, Ye Z, Jang YY. Roles of reactive oxygen species in the fate of stem cells.

- ls. *Antioxid Redox Signal*. 2014;20(12):1881-1890.
52. Owusu-Ansah E, Banerjee U. Reactive oxygen species prime *Drosophila* haematopoietic progenitors for differentiation. *Nature*. 2009;461(7263):537-541.
 53. Ezashi T, Das P, Roberts RM. Low O₂ tensions and the prevention of differentiation of hES cells. *Proc Natl Acad Sci U S A*. 2005;102(13):4783-4788.
 54. Mandal S, Lindgren AG, Srivastava AS, Clark AT, Banerjee U. Mitochondrial function controls proliferation and early differentiation potential of embryonic stem cells. *Stem Cells*. 2011;29(3):486-495.
 55. Holmstrom KM, Finkel T. Cellular mechanisms and physiological consequences of redox-dependent signalling. *Nat Rev Mol Cell Biol*. 2014;15(6):411-421.
 56. Wang K, Zhang T, Dong Q, Nice EC, Huang C, Wei Y. Redox homeostasis: the linchpin in stem cell self-renewal and differentiation. *Cell Death Dis*. 2013;4:e537.
 57. Liang R, Ghaffari S. Stem cells, redox signaling, and stem cell aging. *Antioxid Redox Signal*. 2014;20(12):1902-1916.
 58. Tan SWS, Lee QY, Wong BSE, Cai Y, Baeg GH. Redox Homeostasis Plays Important Roles in the Maintenance of the *Drosophila* Testis Germline Stem Cells. *Stem Cell Reports*. 2017;9(1):342-354.
 59. Wu XW, Lee CC, Muzny DM, Caskey CT. Urate oxidase: primary structure and evolutionary implications. *Proc Natl Acad Sci U S A*. 1989;86(23):9412-9416.
 60. Simons BD, Clevers H. Strategies for homeostatic stem cell self-renewal in adult tissues. *Cell*. 2011;145(6):851-862.
 61. Cieslar-Pobuda A, Yue J, Lee HC, Skonieczna M, Wei YH. ROS and Oxidative Stress in Stem Cells. *Oxid Med Cell Longev*. 2017;2017:5047168.
 62. Shi X, Zhang Y, Zheng J, Pan J. Reactive oxygen species in cancer stem cells. *Antioxid Redox Signal*. 2012;16(11):1215-1228.
 63. Nichols J, Zevnik B, Anastassiadis K, et al. Formation of pluripotent stem cells in the mammalian embryo depends on the POU transcription factor Oct4. *Cell*. 1998;95(3):37

- 9-391.
64. Matic I, Antunovic M, Brkic S, et al. Expression of OCT-4 and SOX-2 in Bone Marrow-Derived Human Mesenchymal Stem Cells during Osteogenic Differentiation. *Open Access Maced J Med Sci*. 2016;4(1):9-16.
 65. Ito K, Suda T. Metabolic requirements for the maintenance of self-renewing stem cells. *Nat Rev Mol Cell Biol*. 2014;15(4):243-256.
 66. Pattappa G, Heywood HK, de Bruijn JD, Lee DA. The metabolism of human mesenchymal stem cells during proliferation and differentiation. *J Cell Physiol*. 2011;226(10):2562-2570.
 67. Ortiz LA, Gambelli F, McBride C, et al. Mesenchymal stem cell engraftment in lung is enhanced in response to bleomycin exposure and ameliorates its fibrotic effects. *Proc Natl Acad Sci U S A*. 2003;100(14):8407-8411.
 68. Chen J, Li Y, Wang L, et al. Therapeutic benefit of intravenous administration of bone marrow stromal cells after cerebral ischemia in rats. *Stroke*. 2001;32(4):1005-1011.
 69. Mahmood A, Lu D, Wang L, Li Y, Lu M, Chopp M. Treatment of traumatic brain injury in female rats with intravenous administration of bone marrow stromal cells. *Neurosurgery*. 2001;49(5):1196-1203; discussion 1203-1194.
 70. Chamberlain G, Fox J, Ashton B, Middleton J. Concise review: mesenchymal stem cells: their phenotype, differentiation capacity, immunological features, and potential for homing. *Stem Cells*. 2007;25(11):2739-2749.
 71. Bartel DP. MicroRNAs: genomics, biogenesis, mechanism, and function. *Cell*. 2004;116(2):281-297.
 72. Su Z, Yang Z, Xu Y, Chen Y, Yu Q. MicroRNAs in apoptosis, autophagy and necroptosis. *Oncotarget*. 2015;6(11):8474-8490.
 73. Lenkala D, LaCroix B, Gamazon ER, Geeleher P, Im HK, Huang RS. The impact of microRNA expression on cellular proliferation. *Hum Genet*. 2014;133(7):931-938.
 74. Szulwach KE, Li X, Smrt RD, et al. Cross talk between microRNA and epigenetic re

- gulation in adult neurogenesis. *J Cell Biol.* 2010;189(1):127-141.
75. Jiang K, Ren C, Nair VD. MicroRNA-137 represses Klf4 and Tbx3 during differentiation of mouse embryonic stem cells. *Stem Cell Res.* 2013;11(3):1299-1313.
 76. Sun G, Ye P, Murai K, et al. miR-137 forms a regulatory loop with nuclear receptor TLX and LSD1 in neural stem cells. *Nat Commun.* 2011;2:529.
 77. He Z, Guo X, Tian S, et al. MicroRNA-137 reduces stemness features of pancreatic cancer cells by targeting KLF12. *J Exp Clin Cancer Res.* 2019;38(1):126.
 78. Xu N, Papagiannakopoulos T, Pan G, Thomson JA, Kosik KS. MicroRNA-145 regulates OCT4, SOX2, and KLF4 and represses pluripotency in human embryonic stem cells. *Cell.* 2009;137(4):647-658.

ABSTRACT (IN KOREAN)
요산에 의한 중간엽 줄기세포의 줄기능 조절
< 지도교수 이 필 휴 >
연세대학교 대학원 의과학과
김 하 나

파킨슨병은 중뇌 흑질에서 도파민성 뉴런이 점진적으로 손실되고 주로 응집된 알파시뉴클레인으로 구성된 단백질피브릴라 세포질 포착물인 루이소체가 존재하는 것이 병리학적으로 특징이다. 질병 치료 전략으로서, 중간엽줄기세포는 신경영양성장인자, 케모카인, 시토카인, 세포외 기질단백질 등 다양한 세포방성인자를 분비해 신경보호 효과를 발휘하기 때문에 파킨슨병의 세포기반 치료의 원천으로서 잠재력이 크다. 중간엽 줄기세포 기반 치료의 가장 큰 당면과제는 자연적인 중간엽 줄기세포 틈새를 모방한 체외 배양 방법을 개발하는 것이다. 세포 프라이밍은 중간엽 줄기세포 운명, 혈통별 차별화, 기능에 대한 접근방식이 유망하며 치료 잠재력도 강화한다. 요산은 강력한 항산화 물질로서 활성산소종을 스캐빈다. 세포 신진대사의 결과로 생성된 활성산소종은 줄기세포를 주성화하고 분화시키는데 중요한 역할을 한다. 본 연구에서 요산이 산화 스트레스에 대한 활성산소종 수준을 효율적으로 낮출 수 있다고 가정했고, 따라서 중간엽 줄기세포의 상태를 유지하는 데 중심적인 역할을 한다. 이를 위해 파킨슨 모델을 이용한 중간엽 줄기세포 프라이밍이 보다 강력한 신경보호 효과를 발휘해 조직공학에서 중간엽 줄기세포 적용을 개선하는 실질적인 전략을 제공하는지 평가했다. 세포 실험에서 중간엽 줄기세포의 요산 처리는 대조군에 비해 PPP의 레벨에는 변화가 없었고 PKM과 LDH의 레벨을 증가시켜 당분해를 자극했다. 저농도의 짧은 요산 배양은 줄기능 조절 관련 전사인자 발현이 현저히 증가했다. 분화배양액으로 중간엽 줄기세포를 분화시킨 후에 요산 처리는 골형성, 지방형성, 연골형성 관련 유전자의 발현을 증가시켰다. 마찬가지로, 요산 상승요법을 받은 동물에서 분리되어 배양된 중간엽 줄기세포는 세포 증식이 증가하였고 세포 노화에는 변화가 없이 줄기능 관련 마커인 OCT4, NANOG, SOX2의 발현이 증가했다. 요산으로 프라이밍한 중간엽 줄기세포는 신경 유도 세포 모델에서 세포사멸 신호경로를 억제하여 신경세포에서 세포생존성을 증가시켰다. MPTP 처리된 생쥐의 도파민성 뉴런에 대한 중간엽 줄기세포의 프로생존 효과는 중간엽 줄기세포가 주입된 생쥐에 비해 프라이밍된 중간엽 줄기세포를 주입한 생쥐에서 운동결손에서 더 나은 행동회복을 보였다. 마지막으로, miR-137과 miR-145의 발현은 대조군과 비교하여 요산 처리된 중간엽 줄기세포에서 상대적으로 줄어든다는 것을 알아냈다. 우리의 데이터는 요산으로 프라이밍한 중간엽 줄기세포가 파킨슨병 모델에서 줄기능과 분화 잠재력을 향상시킴으로써 신경 보호 특성을 발휘하며, 파킨슨병 치료 시 중간엽 줄기세포 적용을 개선할 수 있는 실질적인 전략임을 암시한다.

 핵심되는 말 : 파킨슨병, 중간엽줄기세포, 요산, 프라이밍, 줄기능

PUBLICATION LIST

1. Oh SH, Kim HN, Park HJ, Shin JY, Lee PH. Mesenchymal Stem Cells Increase Hippocampal Neurogenesis and Neuronal Differentiation by Enhancing the Wnt Signaling Pathway in an Alzheimer's Disease Model. *Cell Transplant.* 2015;24(6):1097-1109.
2. Kim YJ, Park HJ, Lee G, et al. Neuroprotective effects of human mesenchymal stem cells on dopaminergic neurons through anti-inflammatory action. *Glia.* 2009;57(1):13-23.
3. Park HJ, Bang G, Lee BR, Kim HO, Lee PH. Neuroprotective effect of human mesenchymal stem cells in an animal model of double toxin-induced multiple system atrophy parkinsonism. *Cell Transplant.* 2011;20(6):827-835.
4. Park HJ, Shin JY, Kim HN, Oh SH, Lee PH. Neuroprotective effects of mesenchymal stem cells through autophagy modulation in a parkinsonian model. *Neurobiol Aging.* 2014;35(8):1920-1928.
5. Park HJ, Shin JY, Lee BR, Kim HO, Lee PH. Mesenchymal stem cells augment neurogenesis in the subventricular zone and enhance differentiation of neural precursor cells into dopaminergic neurons in the substantia nigra of a parkinsonian model. *Cell Transplant.* 2012;21(8):1629-1640.
6. Shin JY, Park HJ, Kim HN, et al. Mesenchymal stem cells enhance autophagy and increase beta-amyloid clearance in Alzheimer disease models. *Autophagy.* 2014;10(1):32-44.